Transactive Control Approach to Trip Optimization in Electric Railways

David D'Achiardi, Eduardo Pilo, Sudip K. Mazumder, and Anuradha M. Annaswamy

***Abstract*— Dynamic trip optimization in electric rail networks is a relatively unexplored topic. In this paper, we propose a transactive controller that includes an optimization framework and a control algorithm that enable minimum cost operation of an electric rail network. The optimization framework attempts to minimize the operational costs for a given electricity price by allowing variations of the trains' acceleration profiles and therefore their power consumption and energy costs. Constraints imposed by the train dynamics, their schedules, and power consumption are included in this framework. A control algorithm is then proposed to optimize the electricity price through an iterative procedure that combines the desired demand profiles obtained from the optimization framework together with the variations in Distributed Energy Resources (DERs) while ensuring power balance. Together, they form to an overall framework that yields the desired transactions between the railway and power grid infrastructures. This approach is validated using simulation studies of the Southbound Amtrak service along the Northeast Corridor (NEC) between Boston, MA and New Haven, CT in the United States, reducing energy costs by 10% when compared to standard trip optimization based on minimum work.**

I. INTRODUCTION

Modern electric trains can both demand power from their traction system for locomotion and inject power back into the electricity network through regenerative braking, virtually enabling them to store electricity in the form of kinetic energy [1]. The power profile of a train along a route is in many cases determined by the conductor based on training and experience, attempting to meet a given schedule with little regard to the varying electricity price along the route. We propose an alternative operation methodology that minimizes electricity costs and coordinates the trains and rail-side distributed energy resources (DERs) along the electric railway through a suitable determination of prices, and schedules of power consumption for the trains and power generation for the DERs. We denote this overall approach as transactive control, as it results in a desired coordination between the rail and power grid infrastructure, similar to the Transactive Energy approach demonstrated in the Olympic Peninsula by PNNL to incentivize grid consumers [2].

In the first part of the proposed transactive control approach, we propose a trajectory optimization framework where a non-convex energy cost is minimized for a given electricity price profile along the track, leading to optimal power energy consumption profiles. The second part is a control algorithm that iteratively determines the electricity price profiles so as to accommodate variations in DERs and other grid-wise operational costs. The overall control approach is shown to reduce energy costs when compared against standard trip optimization that minimizes work in simulation studies. While the methods utilized for solving these two parts are fairly straightforward, the main contribution of the paper lies in the novelty of the proposed approach for trip optimization in electric railway networks. To our knowledge, such a transactive approach, which can be viewed as Demand Response using the flexibility in power consumption of trains, has not been suggested thus far in the literature.

Related work that has addressed trip optimization in rail networks can be found in [3], [4], [5], [6], and [7]. Reference [3] provides a summary of the trajectory planning problem in railway systems. Optimal trajectory planning for electric railways can be found in chapters 3 and 4 of [4], where pseudospectral methods are used to determine optimal railway operation based on models of train dynamics. This work builds upon the work minimization literature developed by [5] and [6]. Finally, [7] develops a control system to reduce fuel use in freight locomotives. In all of these lines of research, the overall objective is to minimize energy use, or work done by the train, rather than the cost of the electricity to the railway operator, an important component of our proposed scheme.

The remainder of this paper is organized as follows. Section II establishes the dynamic model of the train and formulates the energy cost minimization problem. In Section III we develop an iterative market mechanism to determine the electricity prices along the track that dispatch the generators and determine the power profiles of the trains which minimize energy costs. Section IV presents a case study of the Amtrak service along the Northeast Corridor, validating minimum cost operation against the standard minimum work baseline and field data. The simulation environment is extended to test the proposed transactive controller with multiple trains and DERs. Lastly, a conclusion and future research extensions are discussed in Section V.

II. OPTIMIZATION FRAMEWORK

This section describes the physical model of the train in Section II.A. Next, we define the cost minimization problem for a track with multiple pricing regions, or Area Control Centers (ACCs) in Section II.B. This problem will be solved

This work was supported by NSF's Cyber-Physical Systems program under award 1644877.

D. D'achiardi and A.M. Annaswamy are with the Department of Mechanical Engineering, Massachusetts Institute of Technology, Cambridge, MA, 02139 USA $[davidhdp, aanna]$ $@mit.edu$.

E. Pilo is with EPRail Research and Consulting, 28015 Madrid, Spain $eduardo.pilo@eprail.com$.

S. K. Mazumder is with the Department of Electrical and Computer Engineering, University of Illinois at Chicago, Chicago, IL, 60607 USA $mazumder@uic.edu$.

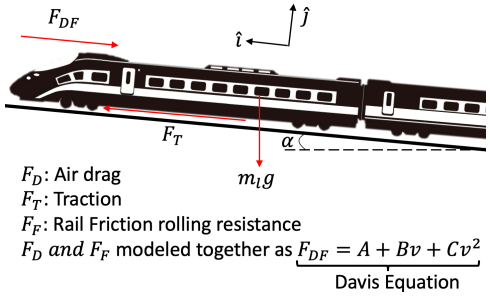

Fig. 1: Free body diagram of electric train l. The resulting traction force F_T, friction and drag force F_{DF} and the gravitational force component in the direction of motion of the train $m_l g sin\alpha$ are identified.

by each train in the railway for the prices derived by the transactive control algorithm developed in Section III and tested through numerical simulation of the Amtrak NEC in Section IV.

A. Dynamic Model of Electric Trains

In order to illustrate the forces acting on the train cars, we develop a free body diagram of the system as shown in 1.

The electric trains are modeled as single bodies with forces that can be decomposed into the direction of motion $\hat{\mathbf{i}}$, in a plane parallel to the rail, and a direction normal to the plane of the ground $\hat{\mathbf{j}}$.

We proceed by defining the three forces with a component in the direction of motion of the train $\hat{\mathbf{i}}$ as it travels at an angle α from the horizon. The total mass of train l is defined as m_l, from which we can describe the gravitational force acting at the center of mass of the train in the direction of the center of the earth as $m_l g$. The gravitational force on the train can be decomposed into the direction of motion $\hat{\mathbf{i}}$ as $-m_l g sin(\alpha)$ and the direction normal to the ground $\hat{\mathbf{j}}$ as $-m_l g cos(\alpha)$. The electric motors convert electrical into mechanical power resulting in the traction force F_T in the $\hat{\mathbf{i}}$ direction.

The air around the train exerts a force throughout the surface of the train assembly as it moves through space which we identify as air drag F_D in the direction opposite to the motion of the train $-\hat{\mathbf{i}}$. Additionally, the rail exerts a friction force F_F against the motion of the train in the $-\hat{\mathbf{i}}$ direction. These two forces will be modeled as a single force using the Davis Drag Equation, and will be identified as F_{DF} henceforth.

Based on the definition of these forces, Newton's second law of motion in the direction of travel of the train $\hat{\mathbf{i}}$ is given as:

$$\sum F_{\hat{\mathbf{i}}} = m_l a_{\hat{\mathbf{i}}} = F_T - F_{DF} - m_l g sin\alpha. \tag{1}$$

The idea of capturing the drag and rail friction components of a train along a level rail using a second-order polynomial dates back to a 1926 publication of the Railway Engineering Department at the General Electric Company authored by W.J. Davis Jr. [8] and is since known as the Davis Equation. For a wide range of train geometries and operational speeds the Davis equation remains the industry standard approximation to the friction and drag forces acting on a train, and is therefore adopted by our model in the following form:

$$\sum F_{DF} = A + Bv + Cv^2. \tag{2}$$

Broadly speaking the A and Bv terms of the Davis Equation capture the rolling resistance of the train which is dominant at low speed. The drag force on the train becomes significant at higher speeds, and is primarily captured by the Cv^2 term.

The dynamics of the train in the direction of motion enter the energy cost minimization problem as constraints. These dynamics introduce the topography of the space traveled through the gradient angle α, which is a central reason why convexity is lost in the optimization problem.

B. Minimum Cost Problem Formulation

In the analysis henceforth, we consider the cost minimization problem of a train l that departs location x_0 at time t_0 and arrives at a final destination x_f at time t_f, making stops at passenger stations denoted by $s\epsilon\{0, ..., f\}$. We capture the kinematics of the train by defining the position $x_l(t)$, velocity $v_l(t)$, and acceleration $a_l(t)$ of the train, which are continuous functions between t_0 and t_f.

The operator must choose the power demand of the train at the nth area control center, denoted as $ACC_n, \forall n\epsilon\{1, ..., N\}$ given by the set of functions $P_l(t, n)\forall t\epsilon[t_0, t_f], \forall n\epsilon\{1, ..., N\}$. The conversion of electric to mechanical power through the train's electric motors results in a traction force profile $F_{T,l}(t)\forall t\epsilon[t_0, t_f]$ which minimizes the cost of the trip. The energy price along the trip may depend on the ACC as well as the time of day and is given by the set of functions $\pi_n(t)\forall t\epsilon[t_0, t_f], \forall n\epsilon\{1, ..., N\}$.

The energy cost minimization of the train can be formulated as:

$$\min_{P_l(t,n)} \quad \sum_{n=1}^{N} \int_{t=t_0}^{t=t_f} P_l(t, n)\pi_n(t)dt \tag{3}$$

$$\text{s.t.} \quad t_{l,arr}(s) \geq t_{l,stop,min}(s), \qquad \forall s\epsilon\{0, ..., f\} \tag{4}$$

$$t_{l,dep}(s) \leq t_{l,stop,max}(s), \qquad \forall s\epsilon\{0, ..., f\} \tag{5}$$

$$P_l(t, n) \geq P_{l,min}(n), \qquad \forall n\epsilon\{1, ..., N\} \tag{6}$$

$$P_l(t, n) \leq P_{l,max}(n), \qquad \forall n\epsilon\{1, ..., N\} \tag{7}$$

$$v_l(t) \geq v_{l,min}(x_l(t)), \qquad \forall t\epsilon[t_0, t_n] \tag{8}$$

$$v_l(t) \leq v_{l,max}(x_l(t)), \qquad \forall t\epsilon[t_0, t_n] \tag{9}$$

$$a_l(t) \geq a_{l,min}, \qquad \forall t\epsilon[t_0, t_n] \tag{10}$$

$$a_l(t) \leq a_{l,max}, \qquad \forall t\epsilon[t_0, t_n] \tag{11}$$

$$F_{T,l}(t) \geq F_{T,l,min}(v_l(t)), \qquad \forall t\epsilon[t_0, t_n] \tag{12}$$

$$F_{T,l}(t) \leq F_{T,l,max}(v_l(t)), \qquad \forall t\epsilon[t_0, t_n] \tag{13}$$

where (3) represents the energy cost incurred by the train across all ACCs between t_0 and t_n.

Constraints (4) and (5) constrain the time spent at the stations to the minimum arrival time $t_{l,stop,min}(s)\forall s\epsilon\{0, ..., f\}$ and the maximum departure time $t_{l,stop,max}(s)\forall s\epsilon\{0, ..., f\}$ respectively.

The power demand of train l from the traction system at each ACC, $P_l(t,n)$, is constrained by (6) and (7) which impose a lower bound at $P_{l,min}(n)\forall n\epsilon\{1,...,N\}$ and an upper bound at $P_{l,max}(n)\forall n\epsilon\{1,...,N\}$. Note that the limits are functions of the ACC in question as the particular track segment might not be able to receive or provide more than a given power magnitude. Changing these limits is one way in which our work could be extended to demand charge management (as discussed in Section V).

The velocity of the train $v_l(t)\forall t\epsilon[t_0,t_n]$ is bound from below by (8) and from above by (9) where the limits are functions of the position $x_l(t)\forall t\epsilon[t_0,t_n]$. This dependency traces back to civil speed limit restrictions which reduce the window of allowed speeds in sections of the track with rail crossings, densely populated areas and passenger stations.

In a similar fashion, the acceleration rate of the train is limited due to safety considerations of the passengers, who may be standing during moments of deceleration (10) and acceleration (11).

Finally, we include limits on the traction force $F_{T,l}(t)$ with (12) and (13) which reduce the feasible traction force window based on the traction force curve of the manufacturer.

In addition to constraints (4)-(13), the trajectory optimization formulation requires that the state of the train (position $x_l(t)$, velocity $v_l(t)$ and acceleration $a_l(t)$) and the dynamic input (traction force $F_{T,l}(t)$) be treated as decision variables in the problem formulation and that the train dynamics described in Section II.A enter the formulation as constraints.

In summary, in this section we have posed the problem of optimizing the power consumption of a train for a time-schedule in the form of a non-convex constrained optimization problem in (3)-(13). The resulting solution is in the form of power demand profiles $P_l^*(t,n)$ for a train l at time t and node n for a given set of price profiles $\pi_n(t)$. This solution may be determined using any one of several commercial software packages such as Matlab's fmincon [9].

III. TRANSACTIVE CONTROL-BASED ACC PRICE

In the previous section, we assumed that the prices were fixed; however, these prices are jointly determined by the demand and supply of the various agents in the electrical grid, including generators, consumers (including railway networks) and utilities, to name a few. In this section we describe a methodology to update the price at each ACC in response to changes in both the power demand of the trains and cost variability of the electric supply system, including changes to the availability of renewable resources due to unexpected weather conditions, fuel price volatility, and the malfunctioning of generators or transmission and distribution lines. This transactive control-based ACC price provides an incentive for the electric trains to modify their operation by iteratively solving the cost minimization problem (3)-(13) with the updated prices.

The market clearing mechanism at each iteration j operates in the same way that a wholesale energy market would: bids from loads (trains $l\epsilon\{1,...,L\}$) and generators (rail-side DERs $g\epsilon\{1,...G\}$) are received at each track pricing region ($ACC_i\epsilon\{1,...,N\}$) for a given time horizon $t\epsilon[t_0,t_f]$ which includes quantity ($P_l(t,n,j)=P_l^*(t,n)$ for the trains and $P_g(t,n,j)$ for the generators) and price components. In the case of the trains, the price portion of the bid is the minimum of the reserve price for serving the route $\pi_{res,l}$ (meaning the price at which the train l would not operate the route because it is prohibitively expensive, which is expected to be very large) and the price of energy sold by the utility or wholesale market $\pi_U(t,n)$. For the systems considered in this analysis, the reserve price for the route is strictly greater than the price of energy sold by the utility or wholesale market ($\pi_{res}>\pi_U(t,n)$). The generators submit the price $\pi_g(t,n,j)$ which is equivalent to the payment they will receive if they clear in the market and is expected to be the opportunity cost of providing power in that interval. Using these bids, the market clears in a least cost fashion, determining the dispatch for each generator, confirming the load served, and a price for that iteration $\pi_n(t_i,j+1)$.

Given that the price calculated for the market is not the price used by the trains in determining their quantity bids, they must re-optimize based on the new pricing information and submit a new quantity bid to the market. If any changes occur in the supply side of the market, these changes must be reflected in the price-quantity information submitted to the ACC in the next iteration. The transactive controller therefore transitions between a quantity and price bid update stage (where the optimization problem (3)-(13) is solved) and an ACC price update stage.

The iterative market clearing terminates once the price at all of the nodes converges to a predetermined level of precision γ. In the simulations developed in Section IV, γ is set to 1%, meaning that the iterative market clearing will terminate at iteration $j+1$ once the price at each node during iteration $j+1$ is within 1% of the price of iteration j.

At each ACC $n\epsilon\{1,...,N\}$ and iteration j of the transactive controller, we require that the aggregation of the loads of the trains $l\epsilon[1,...,L]$ is equal to the sum of the output of the DERs $g\epsilon[1,...,G]$ and the utility U as given by:

$$\sum_{l=1}^{L} P_l(t,n,j) = \sum_{g=1}^{G} P_g(t,n,j) + P_U(t,n,j) \quad \forall n\epsilon\{1,...,N\},\forall j\epsilon\{1,...,J\}. \quad (14)$$

Note that the output of the DERs can be either positive (generation) or negative (load) given that this category also encompasses rail-side storage devices.

Next, we derive a price update rule based on the average cost of energy at each node. For iteration $j+1$ of the controller, the price at node n and time t is given by:

$$\pi_n(t,j+1) = \frac{\int_t^{t+\delta t}\sum_{g=1}^{G} P_g(t,n,j)\pi_g(t,n) + P_U(t,n,j)\pi_U(t,n)dt}{\int_t^{t+\delta t}\sum_{l=1}^{L} P_l(t,n,j)dt} \quad \forall t\epsilon[t_0,t_f],\forall n\epsilon\{1,...,N\},\forall j\epsilon\{1,...,J\} \quad (15)$$

Note that the price $\pi_n(t,j+1)$ is only sufficient to pay each of the generators based on their bid rather than at the price of

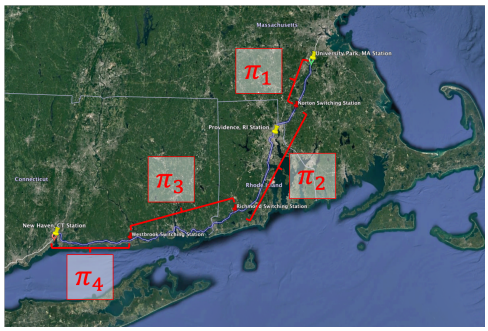

Fig. 2: Map of the four pricing regions identified along Amtrak's NEC between University Park Station in Massachusetts and New Haven Station in Connecticut. This graphic was developed using Google Earth Pro [10].

the last unit that cleared, as is common practice in wholesale energy markets. The overall transactive control algorithm to update the ACC prices is summarized in Algorithm 1.

Algorithm 1 Transactive Control ACC Price

while $|\pi_n(t,j) - \pi_n(t,j-1)| > \gamma \ \exists n \epsilon [1,...,N]$ **do**
  Solve (3)-(13) for power profiles $P_l(t,n,j) = P_l^*(t,n)$ with prices $\pi_n(t,j)$ for each train $l \epsilon [1,...,L]$
  for $n = [1,...N]$ **do**
    Update and sort quantity bids $P_g(t,n,j) \forall g \epsilon [1,...,G]$ & $P_U(t,n,j)$ by their price bids $\pi_g(t,n,j)$ $\forall g \epsilon [1,...,G]$ & $\pi_U(t,n)$
    Solve for minimum cost $P_g(t,n,j) \forall g \epsilon [1,...,G]$ and $P_U(t,n,j)$ in (14)
    Solve for $\pi_n(t,j+1)$ in (15)
  end for
  $j++$
end while.

At the outset, Algorithm 1 is not a standard automatic control solution, but it provides a prescription for determining an electricity price in real-time that best accommodates both consumption-based and generation-based constraints and costs. Such a determination leads to an advantageous interdependency between the rail and grid infrastructures.

IV. Case Study: Amtrak Northeast Corridor

In this section we validate the optimization framework and iterative market mechanism developed in Sections II and III through a case study of Amtrak's NEC. Section IV.A describes Amtrak's services and the parameters used in simulation. In Section IV.B we compare the performance of minimum cost operation against the minimum work standard and a field dataset. Yearly energy cost reductions of minimum cost operation are simulated for Southbound Amtrak Service along the NEC in Section IV.C. Lastly, Section IV.D extends the case study to DER integration along the route, simulating the transactive controller from Section III.

A. Simulation Environment

Once we delved into how electric railway systems are powered, it became evident that the northern Amtrak NEC between Boston, MA and New Haven, CT (within the ISO-NE power system) was well suited for our analysis, as it had four segmented rail power zones that result in the pricing regions identified in Figure 2. The four area control centers, ACC_n identified with $n \epsilon \{1,2,3,4\}$ are powered by the substations at Sharon, MA; New Warwick, RI; London, CT; and Branford, CT respectively and are considered separate pricing regions, each with price $\pi_n \forall n \epsilon \{1,2,3,4\}$.

Amtrak provides two distinct services along the NEC: the high-speed Acela Express and the higher-capacity Northeast Regional. The former utilizes high-speed locomotives developed by Bombardier in the late 1990s based on the French TGV [11]. The latter operates on the Siemens Cities Sprinter ACS-64, introduced in 2014 [12]. Acela Express trains have a total empty weight of $531.2MT$ and a full capacity weight of $556.7MT$. In simulation we assume a partially occupied weight of $m_l = 545MT$. Although the Acela trains are designed to achieve a $264km/h$ top speed, they are limited in operation to $240km/h$ which is equivalent to $v_{l,max} = 66.67m/s$.The maximum train traction power $P_{l,max}$ is $9.2MW$, while regenerative braking is limited in operation to $P_{l,min} = -6.0MW$ [1]. In the absence of public data on the acceleration rates of high-speed trains like the Acela, the estimates used in our simulation ($a_{l,min} = -0.5ms^{-2}$ and $a_{l,max} = 0.5ms^{-2}$) were adopted from models of electric train systems used by EPRail. Fitting the Davis equation (2) to the Acela Express drag and rail friction curve we have that $A = 10,195.16$, $B = 65.81$, and $C = 25.02$.

B. Simulation of Minimum Cost Operation

In the scenario that Amtrak were to face wholesale locational marginal prices (LMPs), for each of its substations, the variability in the LMP differentials along the track and the resulting deviations in the power profile would result in energy cost savings under a minimum cost operation scheme.

For the northern portion of the Amtrak NEC, the wholesale market pricing nodes with the shortest distance to each of the substations (associated with pricing regions π_1 through π_4) were graphically identified as 4123-Cantn, 4813-Blackbrn, 4562-Williams and 4555-Branford respectively. The real-time hourly pricing of calendar year 2016 for each of the four nodes was downloaded from ISO-NE [13]. Using the pricing information of the nodes along the track and the Amtrak Acela Express train timetable [14], we simulate a train following the minimum work and minimum cost operating mode for the schedule with the largest absolute price differences between contiguous ACCs, the 3:10pm South Station departure of Acela 2171 on August 9, 2016.

Matlab's fmincon solver [9] was employed to solve both of these optimization problems, which utilized a Runge-Kutta 4th order multiple shooting collocation routine as implemented by Matthew Kelly's OptimTraj library [15]. We provide a second baseline through a field dataset that was

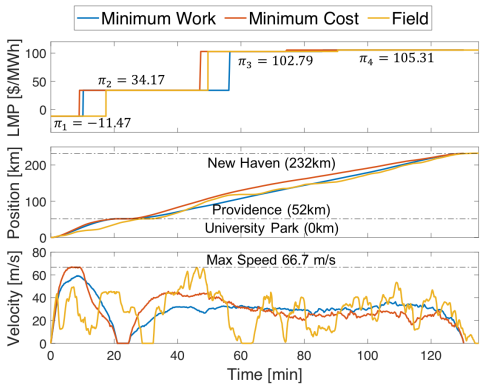

Fig. 3: Plot of LMP [$/Mwh], position [km] and velocity [m/s] against time for the minimum work, minimum cost, and field mode of a southbound trip on Amtrak Acela between University Park Station in MA and New Haven Station in CT with a stop in Providence Station in RI.

collected using the GPS of a mobile phone and the MyTracks iOS application (also for the Acela 2171 schedule, collected on July 1, 2018) [16]. Our results are plotted in Figure 3.

We find that the maximum speed of $66.7 m/s$, and the position datasets are consistent with our field dataset. Minimum work operation reduces cost by 62% from the field estimate (from $\$199.73$ to $\$75.66$) which is in part due to the absence of civil speed limit restrictions along the track which exist at rail crossings, densely populated areas and passenger stations. Most important to our analysis, the train operating under minimum cost can achieve an additional 47% cost reduction when compared to the train operating under the standard minimum work (from $\$75.66$ to $\$40.38$) with a mere 4.8% increase in work (from $1.47 MWh$ to $1.54 MWh$).

Although the ISO-NE real time energy market LMPs of the pricing nodes closest to the feeding substations are used as proxies for electricity costs, the total electricity expenditures are much larger than this value as we neglect the utility's delivery charges, which we include in the yearly cost reduction simulation presented in the next section.

C. Yearly Energy Cost Reductions

As a commercial electricity customer, Amtrak is likely facing retail energy supply and delivery costs, under a utility basic service, rather than participating in wholesale markets. We identify the locations of each substation in the northern portion of the NEC within the service territories of the utilities serving New England, and find that only two feed power to Amtrak, Eversource in MA and CT and National Grid in RI. Although delivery charges include fixed and demand charges, only energy [$/MWh] charges are used in simulation. Based on the location and delivery voltage ($115 kV$), the service at ACC_1 is charged at the Eversource-MA B3 tariff [17] while ACC_2 is served by National Grid-RI under tariff X-01 [18]. The utility and account type is expected to be the same at ACC_3 and ACC_4 (Eversource-CT Rate 58 [19]) and therefore report no supply or delivery charge differential at the boundary.

The yearly energy cost for the minimum work, minimum cost and field train are reported in Table I for each ACC.

Yearly Cost [k\$]	ACC_1	ACC_2	ACC_3	ACC_4	**Total**
Field	413	901	296	565	2,175
Min. Work	353	226	153	223	955
Min. Cost	271	217	158	208	854

TABLE I: Estimated 2018 energy costs for all southbound Amtrak Acela and Northeast Regional trains.

The minimum cost operating mode is able to reduce energy costs based on the energy charges of the retail tariff by 10% when compared to the minimum work operation.

D. Integration of Rail-Side Distributed Energy Resources (DERs)

Building upon the minimum cost simulations under a retail tariff, we consider the opportunity cost of renewable rail-side DERs when injecting power to an ACC as the net energy credit they would otherwise receive for exporting power to the utility. The net energy credits across the year were estimated based on the methodology described by the utilities' fillings with their regulators and are strictly lower than the energy supply and delivery charges. This is consistent with the idea that DERs should not be compensated for costs faced by the utilities that are not offset by exporting power from the site. Consider the electric power generation of two solar arrays, a $600 kW_{AC}$ PV array installed at University Park Station in ACC_1 and a $400 kW_{AC}$ PV array installed at Providence Station in ACC_2. The hourly power output for these two arrays was simulated using NREL's System Advisory Model (SAM) [20]. We assume that the solar facilities generate the power simulated by SAM, and that they use the previous day's generation as their forecast of the day current.

We select an afternoon of Amtrak southbound operations on the northern NEC, June 29, 2018, when two trains, Acela 171 and Northeast Regional 175 are scheduled to stop through University Park Station on route to Washington DC at 3:21pm and 3:32pm respectively. After completing the stop at University Park, they will travel along ACC_1 and transition into ACC_2 around 4pm. The solar arrays have committed their forecast solar power through other contractual mechanisms and now face the challenge of dealing with overgeneration. DER_1 in ACC_1 underestimated its generation by $171 kW$ and DER_2 in ACC_2 underestimated its generation by $53 kW$.

Based on these deviations, we run the transactive controller for the 2 ACCs, which are receiving power requests from the trains, bids from their respective DERs and are subject to the pricing of their associated utilities. The price evolution of each ACC is shown in Table II.

Iteration	π_1 $[\$/MWh]$	π_2 $[\$/MWh]$	$\Delta\ \pi_1[\%]$	$\Delta\ \pi_2[\%]$
1	84.83	85.43	-	-
2	80.39	82.52	-5.2	-3.4
3	80.26	84.00	-0.2	1.8
4	80.43	84.36	0.2	0.4

TABLE II: Evolution ACC prices π_1 and π_2 faced by two southbound trains in response to an increase in solar power availability using the transactive control mechanism developed in Section III.

Within 4 iterations of the transactive controller, the pricing of both ACCs converges to within $\gamma = 1\%$. By incorporating the excess solar power from DER_1 and DER_2 there is an overall cost reduction of 6.8% for an energy usage increase of 3.3% across both of the ACCs and the two trains.

V. CONCLUSIONS AND FUTURE WORKS

Electric trains are a major untapped source of demand-side flexibility in electricity networks. Our findings contribute to the evolution of transportation control systems devoted to work minimization toward higher-level objectives such as the social welfare maximization of joint transportation-electric infrastructures. In particular, our work suggests that the inclusion of time and space varying pricing information modifies the optimal power profiles, yielding reductions in electricity costs for relatively small increases in work.

Fundamentally, this work introduces transactive energy as an additional degree of freedom in the control of a system, which capitalizes on technology advancement (e.g. communication cost reductions, GPS, widespread adoption of regenerative braking) to bridge individual's objectives with those of global infrastructure. This technology could further motivate the deployment of automation technologies in train systems, as the business case improves when factoring electrical cost reductions. We expect that our findings could be developed into a software package for train operators, similar to GE's Trip Optimizer technology which has been adopted by heavy haul train operators to decrease fuel use [7]. There are several key research directions we would like to explore in future work that are briefly described below.

1) Dynamic Market Mechanisms: The transactive control mechanism developed in Section III adopts a simple pricing strategy and iterative market clearing based on the average cost of energy at each ACC. We expect that Dynamic Market Mechanisms such as those proposed in [21] will improve convergence and efficiency of transactive retail markets.

2) Demand Charge Management: Although our work is a step towards including the electric system's costs for a given power profile, we only reflect energy-related costs $(\$/MWh)$. In reality the train operator will also incur demand charges $(\$/MW)$. A means of achieving demand charge management is to update constraints within the optimization problem, modifying the minimum and maximum power limits $P_{l,min}(n)$ and $P_{l,max}(n)$ in (6) and (7) respectively.

3) Regulation and Reserve Market Participation: Similar to the research direction regarding demand charges, we would like to extend the services provided by the transactive control system to the electrical network beyond energy and onto products for frequency regulation and operational reserves. Practical limitations of providing these services as well as the incentive and compensation mechanisms remain to be explored.

REFERENCES

[1] J. Yu and M. B. Ercolino, "Measurement and analysis of acela express regenerative power recovery," in *ASME/IEEE 2007 Joint Rail Conf.* American Society of Mechanical Engineers, pp. 241–248.

[2] R. Melton, "Pacific northwest smart grid demonstration project technology performance report volume 1: Technology performance," Pacific Northwest National Lab. Richland, WA, USA., Tech. Rep., 2015.

[3] Y. Wang, B. Ning, F. Cao, B. De Schutter, and T. J. van den Boom, "A survey on optimal trajectory planning for train operations," in *2011 IEEE Int. Conf. Service Operations, Logistics, and Informatics (SOLI)*. IEEE, pp. 589–594.

[4] Y. Wang, B. Ning, T. Van den Boom, B. De Schutter *et al.*, *Optimal trajectory planning and train scheduling for urban rail transit systems*. Springer, 2016.

[5] E. Khmelnitsky, "On an optimal control problem of train operation," *IEEE Trans. Autom Control*, vol. 45, no. 7, pp. 1257–1266, 2000.

[6] R. Franke, P. Terwiesch, and M. Meyer, "An algorithm for the optimal control of the driving of trains," in *Proc. 39th IEEE Conf. Decision and Control (CDC)*, vol. 3. IEEE, 2000, pp. 2123–2128.

[7] D. Eldredge and P. Houpt, "Trip optimizer for railroads," in *The Impact of Control Technology*, T. Samad and A. Annaswamy, Eds., 2011. [Online]. Available: http://www.ieeecss.org/sites/ieeecss.org/files/documents/IoCT-Part2-20TripOptimizer-LR.pdf

[8] W. J. Davis, *The tractive resistance of electric locomotives and cars*. General Electric, 1926.

[9] T. M. Inc., "Matlab optimization toolbox," Software, 2014.

[10] G. LLC. Google earth pro v 7.3.2.5491. data sio, noaa, us navy, nga, gebco, ldeo-columbia, nsf. image landsat, copernicus. [Online]. Available: http://www.earth.google.com

[11] B. Transportation, *Bombardier High-Speed Trainsets*, 1101 Parent Street, Saint-Bruno, Québec, Canada J3V 6E6, November 2001.

[12] S. R. S. Division, *Amtrak Cities Sprinter ACS-64 Electric Locomotive*, Siemens AG, Nonnendammallee 101 13629 Berlin, Germany, 2014.

[13] ISO New England. (2017, 10) Pricing reports: Final real-time hourly lmps. [Online]. Available: https://www.iso-ne.com/isoexpress/web/reports/pricing/-/tree/lmps-rt-hourly-final

[14] Amtrak, "Amtrak system timetable," National Railroad Passenger Corporation, One Massachusetts Ave., N.W., Washington, DC 20001, Tech. Rep., June 2018.

[15] M. Kelly. (2018, May) optimtraj matlab library v 1.6. [Online]. Available: https://la.mathworks.com/matlabcentral/fileexchange/54386-optimtraj-trajectory-optimization-library

[16] D. Stichling, "mytracks - the gps-logger v 5.0.4," iOS Application, May 2018.

[17] Eversource. (2018) 2018 summary of eastern massachusetts electric rates for greater boston service area. [Online]. Available: $https://www.eversource.com/content/docs/default-source/rates-tariffs/ema-greater-boston-rates.pdf$

[18] N. Grid. (2018, August) Electric propulstion rate (x-01). [Online]. Available: $https://www.nationalgridus.com/media/pdfs/billing-payments/tariffs/ri/x01_ripuc_2194.pdf$

[19] E. Energy. (2018) Electric service rate 58. [Online]. Available: $https://www.eversource.com/content/docs/default-source/rates-tariffs/rate-58-ct.pdf$

[20] National Renewable Energy Laboratory. (2017, 10) System advisor model v 2017.9.5. [Online]. Available: https://sam.nrel.gov/content/downloads

[21] D. J. Shiltz, M. Cvetković, and A. M. Annaswamy, "An integrated dynamic market mechanism for real-time markets and frequency regulation," *IEEE Trans. Sustainable Energy*, vol. 7, no. 2, pp. 875–885, 2016.